Classical solutions of an electron in magnetized wedge billiards

A. Góngora-T,[1,2] Jorge V. José,[2] and S. Schaffner[2]
[1] *Centro de Ciencias Físicas, Universidad Nacional Autónoma de México, Apartheid Postal 48-3, 62250 Cuernavaca, Morelos, Mexico*
[2] *Physics Department and Center for the Interdisciplinary Research on Complex Systems, Northeastern University, Boston, Massachusetts 02115*
(Received 23 April 2002; published 4 October 2002)

We have studied the classical solutions of a free electron constrained to move inside a circular wedge of angle θ_w, in the presence of a homogeneous constant magnetic field B. These billiards have broken rotational symmetry. As B and θ_w are varied, the apex of the billiards affects the classical dynamics in an important way. We find that for billiards with angles $(\sqrt{5}-1)/2 \leqslant \theta_w \leqslant \pi/2$, the dynamics exhibits a *reentrant* transition as the field increases. The transition is from *regular-to-mixed-to-chaotic-to-mixed-to-chaotic regimes*. The reentrance is connected to the appearance and disappearance of periodic orbits nucleated at the boundaries of these billiards as the field increases. There is *no* reentrance when $\theta_w > \pi/2$. In the latter case as B increases the dynamics goes from quasiintegrable, to intermediate and then to chaotic whispering gallery Larmor modes.

DOI: 10.1103/PhysRevE.66.047201 PACS number(s): 05.45.−a, 03.65.−w, 72.20.Ht

Significant progress has been made in the last two decades to understand the emergence of chaotic classical behavior and its quantum counterpart [1–5]. Two-dimensional billiards have played a very important role in the development and understanding of the extreme limits of complete integrability, e.g., occurring in the circular disk billiard, and complete generic chaos in stadium billiards [5]. These billiards have also been studied experimentally in microwave cavities [5] and in electronic mesoscopic billiards [6]. One variant examined in this paper involves removing a sector from an otherwise rotationally invariant circular disk [7,8]. A wedge that has an angle θ_w larger than π is called a pacman billiard, and if it is smaller than π, a sector billiard. The electronic response of triangles [9] and, in particular, of pacmen with a finite width radial bar removed in the center under transverse constant magnetic fields [7,8], have been studied experimentally. There are also early theoretical studies of a charged particles in planar *smooth* boundaries in a constant magnetic fields [10–13]. In this paper we analyze the classical dynamics of sectors and pacmen billiards with different angles in homogeneous magnetic fields. Open wedge billiards in a gravitational field have been studied theoretically by Szeredi and Goodings [14] and more recently experimentally [15]. In the zero magnetic field case we found [16] that the quantum problem has arbitrary *fractional* angular momentum solutions as a function of θ_w. Here we analyze the changes produced by a homogeneous magnetic field. In a future paper we will consider the corresponding quantum problem.

To characterize the transition between the different magnetic dynamical regimes we introduce a "frustration parameter" F; Take r_w the radius of the wedge and $l_B = -Mv/qB$ the Larmor radius, where v is the velocity, M the mass, and q the electron charge. Then $F = [area(full\ circle)]/[area(larmor\ circle)] = (r_w/l_B)^2$. Note that we have defined F in terms of the entire billiard area, since it is more convenient when comparing different wedges of the same circular billiard. The presence of the field breaks time reversal invariance and the wedge geometry breaks rotational invariance. We analyze the dynamics for different F values by looking at specific configuration space trajectories. We compute the Poincaré-Birkhoff (PB) surfaces of section for each one of the cases considered, as well as their corresponding average Lyapunov exponents. The outline of the paper is as follows: In Sec. II we define the model and the approach we introduce to geometrically calculate the dynamical solutions. In Sec. III we present the bulk of our results for the different pacmen and sector wedges and magnetic fields. Finally in Sec. IV we briefly state our main conclusions.

The model

Consider a wedge cut from a circular disk with radius r_w and angle θ_w. The particle moves at a constant velocity along arcs of Larmor circles with radius l_B, and it has elastic collisions with the wedge walls. We use polar coordinates (ρ,θ) with the origin at the apex of the wedge billiard and with $\theta=0$ pointing horizontal along the center of the wedge. The particle is free to move within $-\theta_w/2 \leqslant \theta \leqslant \theta_w/2$ and $0 < \rho < r_w$. The particle has the velocity (v_ρ, v_θ) when it encounters the maximum radius of the wedge. The normal to the outer circle is perpendicular to $\hat{e}_\theta$, so v_θ is unchanged by the collisions. Because the collisions are elastic, the energy $(m/2)[v_\rho^2 + (r v_\theta)^2]$ is constant. This requires that $v_\rho \Rightarrow -v_\rho$. Similarly, for a collision with a wedge radial wall, $(v_\rho, v_\theta) \Rightarrow (v_\rho, -v_\theta)$. The geometry of the trajectory is not changed by a scaling of time or radius (with proper adjustments to the magnetic field B). Thus we can use dimensionless coordinates where $r_w = 1$ and $|\vec{v}| = 1$. In the low-field limit, $F \ll 1$, the oriented trajectory sections are almost straight lines and become parts of chords of the circle in which the wedge is embedded. The regular pattern of bounces of the outer perimeter is disturbed by the reversals of direction from bounces of the side walls. The latter bounces can be removed by constructing an infinite covering space containing a sequence of copies of the wedge. This covering space is constructed by lifting copies of the wedge onto an infinite spiral in θ. Adjacent copies on the spiral are reflections of the area of the actual wedge. When the trajectory of the particle is lifted onto this covering space, each bounce with a sidewall is replaced by a smooth transi-

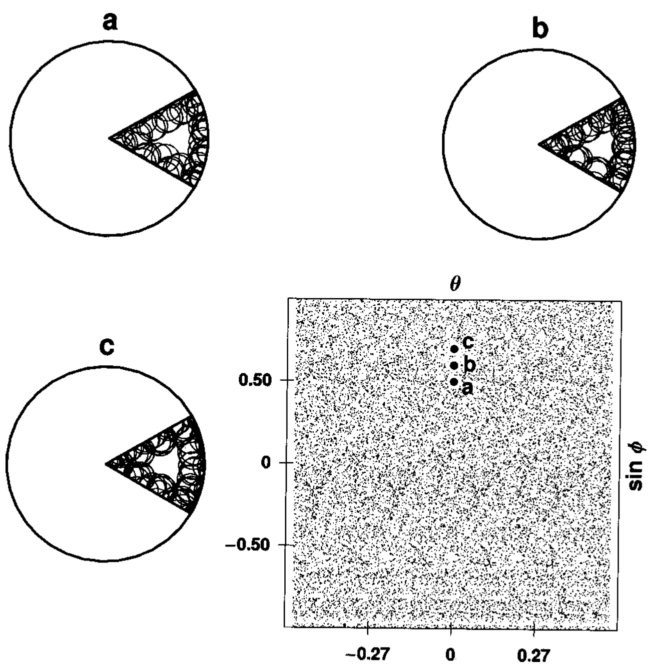

FIG. 1. This figure shows results for a $\pi/3$ sector billiard embedded in the drawn full circle with an $F=50$. The trajectories in configuration space are shown in panels (a–c), for initial conditions with $\theta=0$ and $\sin\phi$ equal to (a) 0.5, (b) 0.6, and (c) 0.7, respectively. The last figure shows the Poincaré-Birkhoff (PB) surface of section for the same initial conditions, plus one more with $\sin\phi=0.8$. Here we note the clear presence of Larmor chaotic whispering gallery modes (LCWGM).

tion into an adjacent wedge copy. Thus only the bounces with the outer periphery remain and the trajectory on the covering space consists of a series of chords at equal angle increments on the spiral. The trajectories will be repeating strictly if θ_w and the chord angle θ_c are commensurate, $q\theta_c=p2\theta_w$, where p and q are relative primes and both are positive [17]. In general, if $\theta_c/2\theta_w=p/q$, where p and q are relatively prime, this corresponds to a (p,q) periodic closed orbit, where the particle bounces p times off the periphery and traverses $2\times q$ copies of the wedge before the trajectory closes.

For the zero-field case, the angle ϕ between the chord as the particle meets the circular boundary and the normal to that periphery determines the angle subtended by the chord. The range $0\leqslant\phi\leqslant\pi/2$ denotes counterclockwise motion and $-\pi/2\leqslant\phi<0$ clockwise. We use $\sin\phi$ instead of ϕ, since it is proportional to the transverse angular momentum $r\sin\phi$ in the full circle ($\sim\vec{r}\wedge\vec{v}$) and together with θ they can be used as the Birkhoff conjugate dynamical variables. Note that once a particle bounces off the boundary, it will always return to the boundary to bounce again before completing a full 2π-rotation in the magnetic field. For high fields, $F\gg1$, a particle will chaotically bounce about the boundary. We call these skipping orbit trajectories "Larmor chaotic whispering gallery modes" (LCWGM).

Results

We start by considering the surface of section and configuration space orbits. We have taken four typical initial

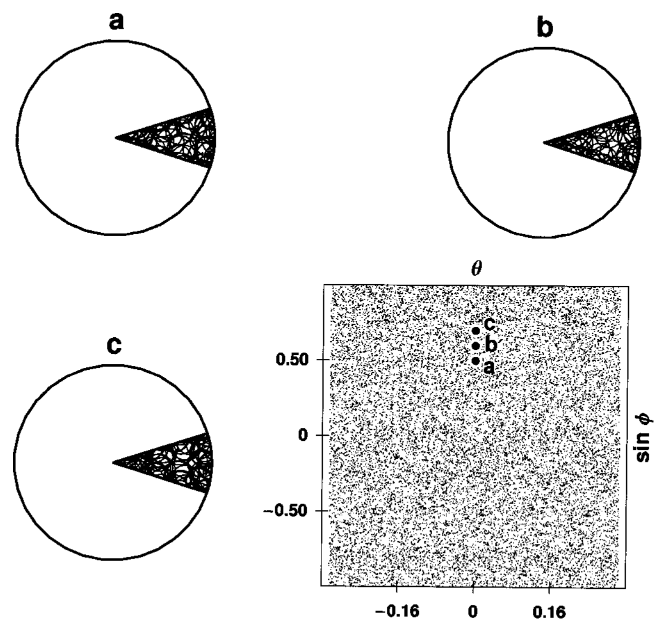

FIG. 2. Here we show results for the α sector in a field of $F=50$ with the same initial conditions as in the previous figure.

conditions to carry out the calculations. They are $\sin\phi_0=0.5$(a), 0.6(b), 0.7(c), and 0.8(d). We start discussing results for two typical angles, $\pi/3$, and the golden mean α, where $\alpha\equiv(\sqrt{5}-1)/2$ is approximated by its computer precision expression. For a very weak magnetic field ($F=\frac{1}{6}\times10^{-6}$) the trajectories are periodic and almost indistinguishable from the zero magnetic field case, except for the fact that they have a definite orientation. The orbits are closed only if the chord length is commensurate with the wedge angle. An interesting case corresponds to the $\theta_w=\pi/3$ with $\sin\phi_0=0.5$, that yields an equilateral triangle orbit. The orbit is closed because $\phi=\pi/6$ and thus the zero-field chord angle, $\theta_c=\pi-2\phi=2\pi/3$, is commensurate with the wedge angle $\theta_w=\pi/3$. There is a small precession on θ

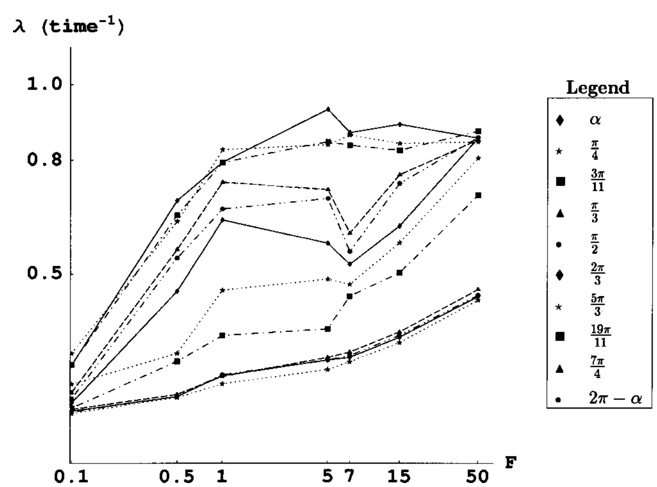

FIG. 3. Lyapunov exponent λ as a function of F for different billiard angles. Note the minimum in λ vs F for $\alpha\leqslant\theta_w\leqslant\pi/2$. Other billiards in contrast have a monotonic increase of λ as a function of F. See text for a full description of this figure.

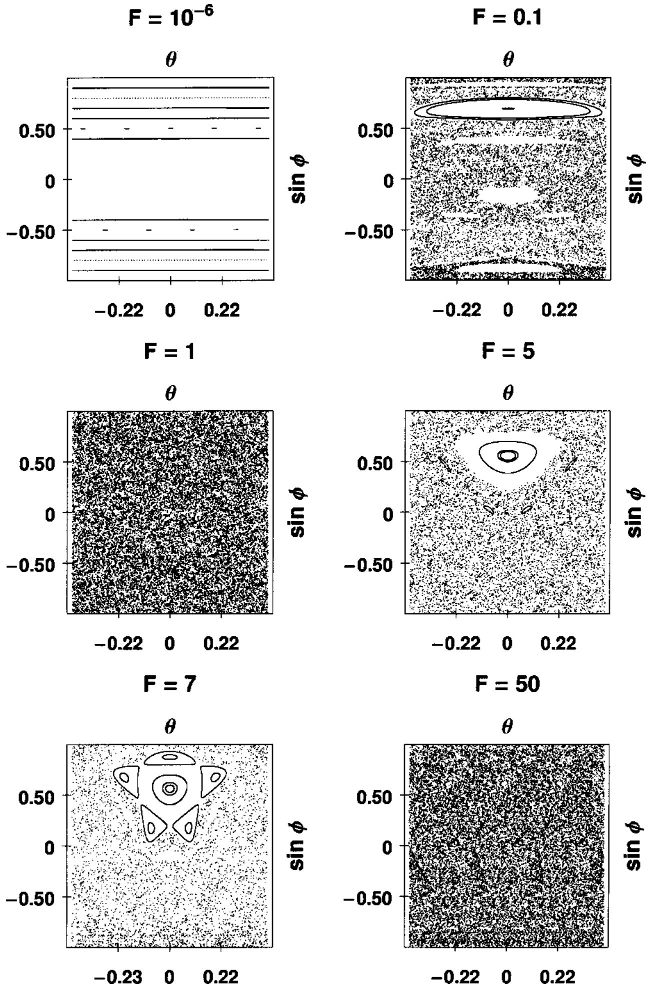

FIG. 4. PB sections for the sector billiard with angle $3\pi/11$, for initial conditions $(\theta_0, \sin\phi_0)$=(0.25,0.4), (0.0,0.5), (0.0,0.6), (0.0,0.7), (0.0,0.8), and (0.0,0.9). Note the reentrant behavior for fields from $F=0.1$ to $F=7$, and again the reemergence of full chaos for $F=50$.

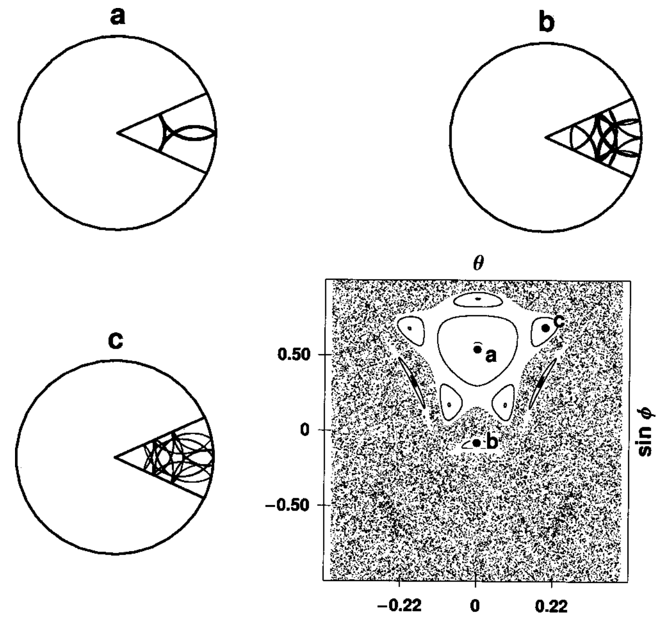

FIG. 5. Configuration space trajectories specifically for $F=7$ and wedge angle $3\pi/11$. The panels (a–b) denote the orbits shown in the PB sections. We have a nucleation of periodic orbits emerging from the sea of chaos. See text for further discussions of this figure.

because of the nonzero magnetic field that slightly perturbs the zero-field chord angle θ_c. For all angular values in a very small field the orbits are integrable in nature with clear caustics for initial conditions (a) and (c). In those cases the PB sections are still made of horizontal lines, which mean that angular momentum for this field is still basically conserved.

As the field increases, many of the orbits become approximately chaotic. For these orbits, it is still useful to assign (p,q) values. It is possible, however, for p and q to be relatively nonprime because the chord lengths vary according to the starting angle θ_0. In Fig. 1 we show results for a higher magnetic field, $F=50$, in the $\pi/3$ sector. In this case we clearly see that for the initial conditions considered lead to the LCWGM. The particle moves around the boundary and the orbits have radii that are smaller than the wedge radius. In the PB sections we see a completely irregular behavior. In Fig. 2 we show the corresponding results for the irrational α sector. In this case the LCWGM are not clearly present nor as well defined as in the $\pi/3$ sector for $F=50$. Next we discuss the pacmen cases for $F=50$. For this F we have that $l_B \leqslant \frac{1}{7}$ of the wedge radius, definitely in the high-field regime. The orbits can be separated into bulk and boundary trajectories. The bulk trajectories are standard free space Larmor closed orbits that do not touch the wedge boundary. The second more interesting type of orbits are the chaotic LCWGM orbits that are formed by small circular arcs that rotate around the boundary. Note that if we increase the field further, as long as an orbit touches the boundary once, it will be generally chaotic due to the apexes in the wedge billiards. For the pacman with initial conditions (a–b) and angle $5\pi/3$, we find complete LCWGM that move about the boundary. The situation is different in case (c). In this case the particle moves in a series of small arcs about the boundary of the wedge. The sizes of the arcs change only when the particle interacts with one of the three boundary discontinuities: one at the apex and two at the outer ends of the wedge walls.

Lyapunov exponent results: Reentrance

In Fig. (3) we show our results for several sector angles; $\alpha, \pi/4, 3\pi/11, \pi/3$, $\pi/2$ and pacmen angle complements of $2\pi/3, 5\pi/3, 19\pi/11, 7\pi/4$ and the irrational complement $2\pi-\alpha$. There we see that the Lyapunov exponent as a function of F is positive definite for values of $F \geqslant 0.1$ indicating that the field breaks integrability fully in both the sectors and pacmen. Note a remarkable minimum for the sectors with angles in the window $\alpha \leqslant \theta_w \leqslant \pi/2$. Such reentrance is not seen in wedges with angles outside of this window. Note that the sectors are more chaotic than the pacmen, measured by the magnitude of the Lyapunov exponent. This makes the reentrance more surprising since the periodic orbits emerge from a sea of stronger chaos appearing in the window of sector angles. A possible reason for this difference and the quasiregularity reentrance is that special orbits can nucleate out of the chaotic sea as the field increases.

To further analyze this situation we decided to look at the PB surfaces of section for the sector with angle $3\pi/11$ as a function of field with $F=10^{-6}$, 0.1, 1.0, 5.0, 7.0, and 50. In this case the initial conditions were $(\theta_0, \sin\phi_0)$=(0.25, 0.4), (0, 0.5), (0, 0.6), (0, 0.7), (0, 0.8), and (0, 0.9). In Fig. 4 we clearly see the transition from integrable to chaotic when F goes from 1 to 5, and then for $F=7$ there are higher periodic orbits, indicated by elliptic islands with positive values of $\sin\phi$. As the field increases further the dynamics become fully chaotic again. These results led us to consider the specific orbits responsible for this reentrant transition in the cases considered. In Fig. 5 we show in panels (a–c) the transformation of the basic fish–like orbit in (a). This orbit is a modification of the zero-field (1,1) orbit. That orbit gets convoluted as the initial conditions change and they are represented by the elliptic regions in the PB panel in the figure.

Thus we see that the region of reentrant stability is based on the (1,1) orbit and a few simple multiples. For small field values, a (1,1) orbit corresponds to a simple circulation within the wedge. For $F=7$, this simple loop has folded over once so that it covers less area. This orbit *completely* disappears and then reappears as F increases. There is no evidence that the reentrant transition is period doubling generated.

In conclusion, we have studied the classical dynamics of a charged particle in the presence of a constant homogeneous magnetic field constrained to move inside a wedge billiard. In this problem the Hamilton-Jacobi equation is not separable. The competition between the rotational invariance of the magnetic field and the breaking of this symmetry in the wedges, plus the presence of the apexes in the billiards, produces the chaotic orbits. We have found a reentrant dynamical transition in sector billiards with angles smaller than $\pi/2$, that is directly connected with the existence of particular orbits that reappear at weak fields. The boundary conditions play a fundamental role in the appearance of this reentrant transition.

For higher fields, the Larmor radius is much smaller than the wedge radius. A particle will continue to touch a wall if it has already touched a wall. The apexes in the billiards play an important role in producing the Larmor chaotic whispering gallery modes at large fields. Our initial motivation to study wedge billiards came from transport experiments on pacman like billiards. From the results presented here we see that there are new effects that can be studied experimentally. To make a direct connection with experiment we need to treat the quantum problem. We shall address the quantum problem in a future publication.

The work by A.G.T. was supported in part by CONACYT and UNAM, México. J.V.J. thanks NSF for partial financial support.

[1] M. C. Gutzwiller, *Chaos in Classical and Quantum Mechanics* (Springer-Verlag, Berlin, 1990).

[2] A. J. Lichtenberg and M. A. Lieberman, *Regular and Chaotic Dynamics,* Applied Mathematical Sciences Vol. 38 2nd ed. (Springer-Verlag, New York, 1992).

[3] G. Casati and C. Chirikov, *Quantum Chaos, between order and disorder* (Cambridge University Press, Cambridge, UK, 1995).

[4] M. J. Giannoni, A. Voros, and J. Zinn-Justin, in *Chaos and Quantum Physics,* Proceeding of the Les Houches Summer School, Session 52 (North-Holland, Amsterdam, 1991), Vol. 52.

[5] H. J. Stöckman, Quantum Chaos an introduction (Cambridge University Press, Cambridge, U.K., 1999), and references therein.

[6] C. M. Marcus *et al.,* Phys. Rev. Lett. **69**, 506 (1992).

[7] M. J. Berry II, *et al.*, Phys. Rev. B **50**, 17 721 (1994).

[8] M. J. Berry II, Ph.D. thesis, Harvard University, 1994.

[9] P. Boggild *et al.,* Phys. Rev. B **57**, 15 408 (1998).

[10] M. Robnik and M. V. Berry, J. Phys. A **18**, 1361 (1985).

[11] J. D. Meiss, Chaos **2**, 267 (1992).

[12] J. Blaschke, and M. Brack, Phys. Rev. A **56**, 182 (1997).

[13] N. Berglund and H. Kunz, J. Stat. Phys. **83**, 81 (1996).

[14] T. Szeredi and D. A. Goodings, Phys. Rev. E **48**, 3518 (1993).

[15] V. Milner *et al.*, Phys. Rev. Lett. **86**, 1514 (2001).

[16] A. Góngora-T., J. V. José, S. Schaffner, and P. H. E. Tiesinga, Phys. Lett. A **274**, 117 (2000).

[17] R. W. Robinett, J. Math. Phys. **39**, 278 (1998).